

Image Quality at Gemini South Observatory

Javier Fuentes Lettura¹, Fredrik Rantakyrö¹

¹NSF's National Optical-Infrared Astronomy Research Laboratory, Gemini Southern Center, Av. Juan

Cisternas 1500, Casilla 603, La Serena, Chile.

E-mail: javier.fuentes@noirlab.edu, fredrik.rantakyro@noirlab.edu

Summary

We present a detailed analysis looking for temporal variation of the optical image quality and seeing measurements from different systems over 18 years at **Gemini South Observatory**. The main findings are highlighted as follows:

- The median **Delivered Image Quality (DIQ)** airmass corrected at 500-nm derived from long-exposure GMOS-S imaging data is 0.75 arcsec.
- DIMM and MASS data** indicate a median seeing at **Cerro Pachón (CP)** of $\varepsilon_0 = 0.76$ arcsec and a median free – atmosphere seeing $\varepsilon_f = 0.46$ arcsec (all layers above 500 m). This result is better to the median $\varepsilon_0 = 0.95$ arcsec and $\varepsilon_f = 0.55$ arcsec as measured by DIMM and MASS in Cerro Tololo Inter-American Observatory (Tokovinin et al. 2002) and very similar and consistent with previous studies conducted in Tololo site during four years of optical monitoring campaigns, see Els et al. (2009).
- MASS data** indicate that a strong annual variation of high-altitude turbulence with the weakest turbulence encountered while approaching the southern summer months.
- The Gemini Wave Front Sensors** follow the trend of the temporal seeing variations. Both GMOS On Instrument Wave Front Sensor (**OIWFS**) and Peripheral Wave Front Sensor 2 (**PWFS2**) underestimate the true seeing. The reason for this discrepancy might have multiple factors, one could be due to either for uncorrected noise bias or guiding loop frequency or both leading to the computation of the seeing value from the captured circular buffers be lower. Another important key correction is for the turbulence outer scale, L_0 .
- Weather influence on the DIQ at Gemini South (GS)**. The DIQ significantly deteriorates when the wind speed is above 5 (m/s) and when the telescope is pointing in southern directions. We believe that the azimuth dependence on winds is a local effect caused by the topography of mountains but the global conditions may play an important role as well as the wind dynamics on the telescope enclosure.

Wave Front Sensors

OIWFs and PWFS seeing:

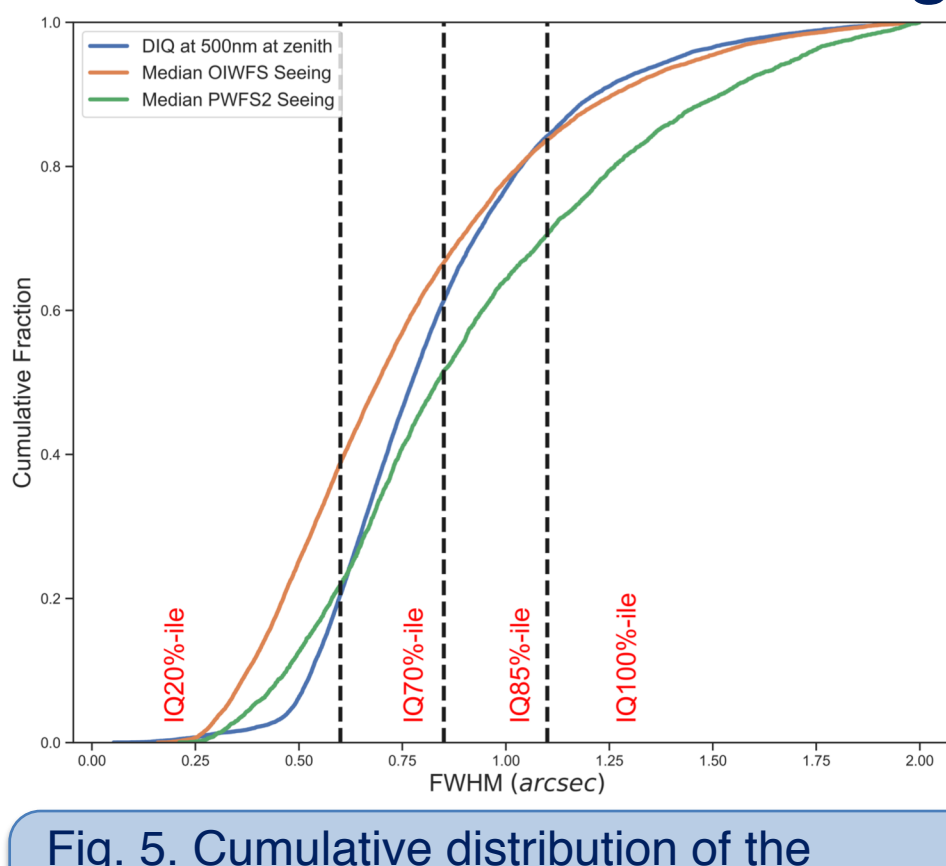


Fig. 5. Cumulative distribution of the GMOS Instrument Wave Front Sensors (OI/P2) and Image FWHM (2014-2022).

| Percentile | DIQ | OIWFS | PWFS2 |
|-------------------------|--------|--------|--------|
| 10 | 0.53'' | 0.38'' | 0.47'' |
| 25 | 0.63'' | 0.50'' | 0.63'' |
| 50 | 0.77'' | 0.69'' | 0.83'' |
| Average | 0.83'' | 0.76'' | 0.92'' |
| 75 | 0.98'' | 0.96'' | 1.18'' |
| 90 | 1.21'' | 1.26'' | 1.52'' |
| Total number of samples | 15,948 | 12,121 | 3,827 |

Table 2. Cumulative statistics of FWHM of long-exposure stellar images ($t \geq 30$ sec) obtained from GMOS DIQ and GMOS (OIWFs/PWFS2) over 8 years (2014-2022).

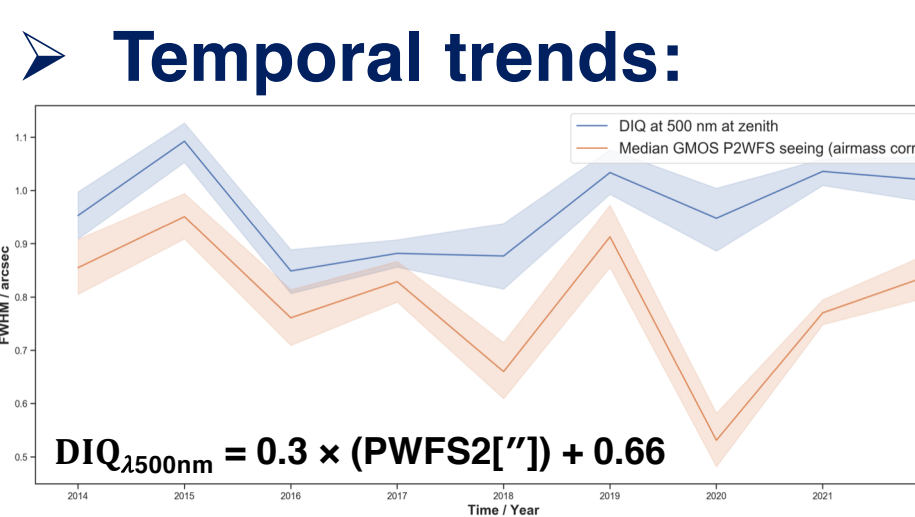


Fig. 6. Temporal line of the DIQ against the GMOS instrument WFS (2014-2022).

Gemini Wave Front Sensors follow the same seeing variations and trends along time as the DIQ measured over GMOS imaging data, but both OIWFS and PWFS2 underestimate the seeing.

Turbulence parameters

Seasonal variations:

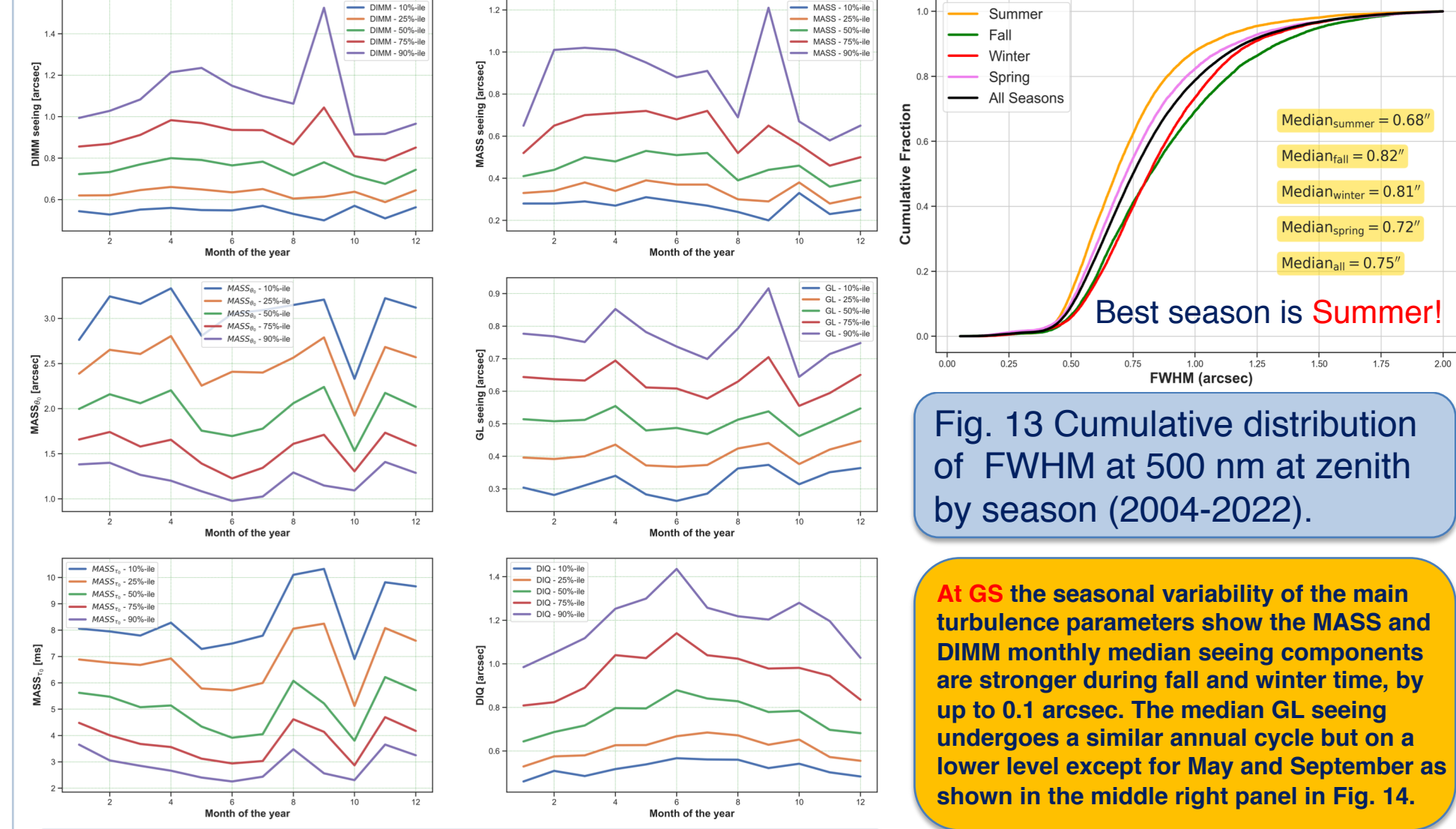


Fig. 13. Cumulative distribution of FWHM at 500 nm at zenith by season (2004-2022).

At GS the seasonal variability of the main turbulence parameters show the MASS and DIMM monthly median seeing components are stronger during fall and winter time, by up to 0.1 arcsec. Median GM seeing undergoes a similar annual cycle, but on a lower level except for May and September as shown in the middle right panel in Fig. 14.

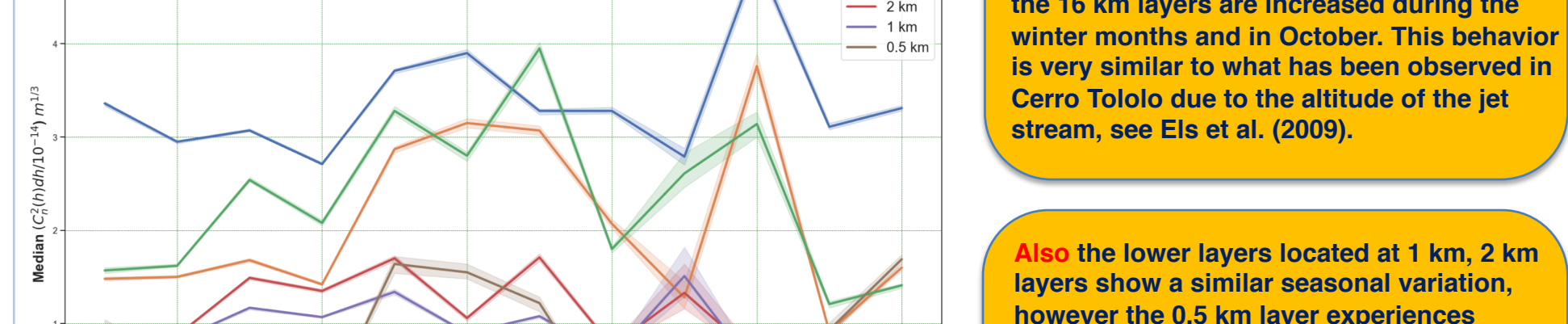


Fig. 14. Main turbulence parameters during the year.

Temporal trends:

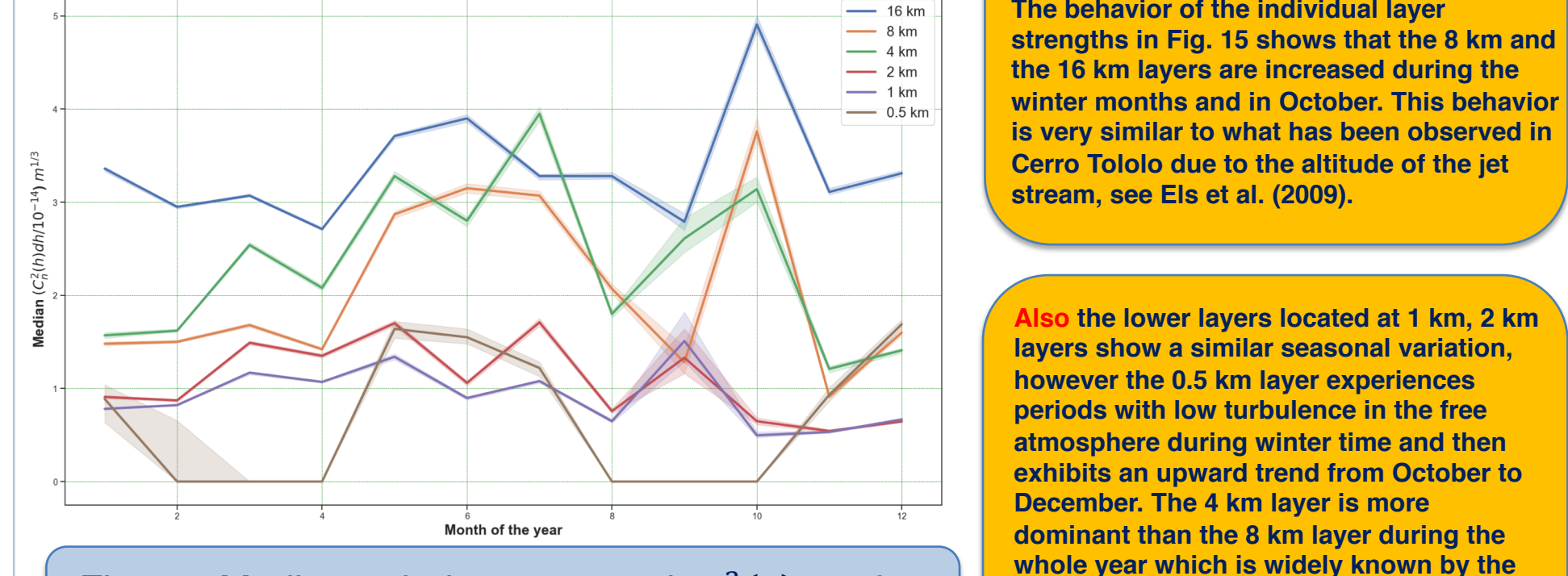


Fig. 15. Median turbulence strength $C_2^2(h)dh$ of the individual MASS layers during the year.

DIQ vs. weather

Wind speed and direction influence on the DIQ:

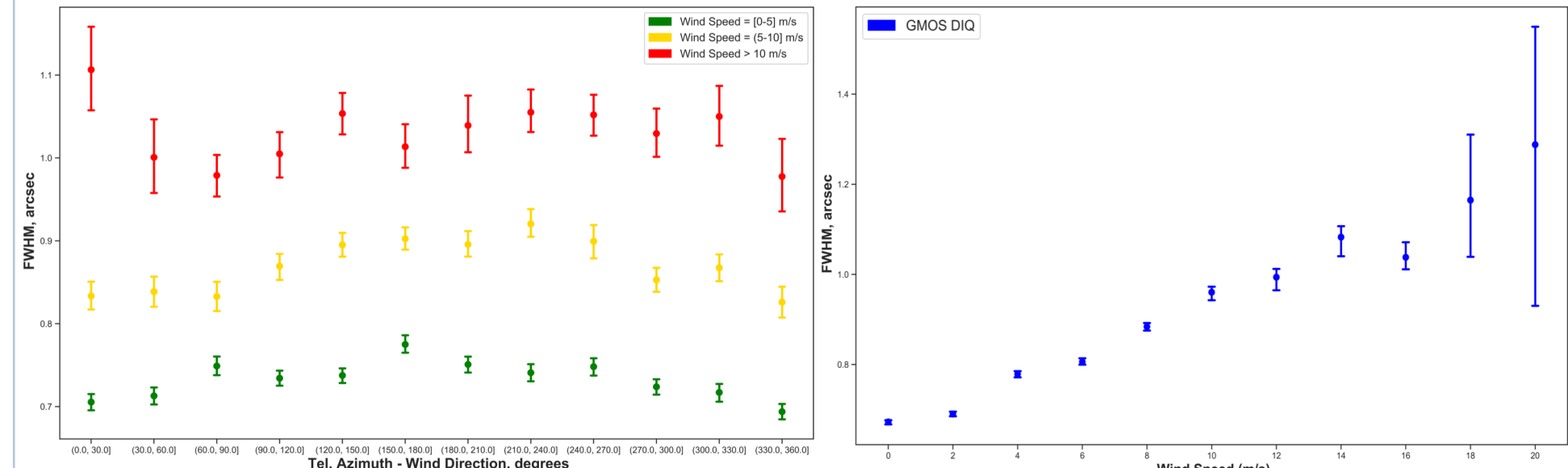


Fig. 16. The DIQ obtained in GMOS images as a function of the telescope azimuth position, incoming winds direction and intensity.

Fig. 17. The DIQ obtained by the telescope as a function of the wind speed.

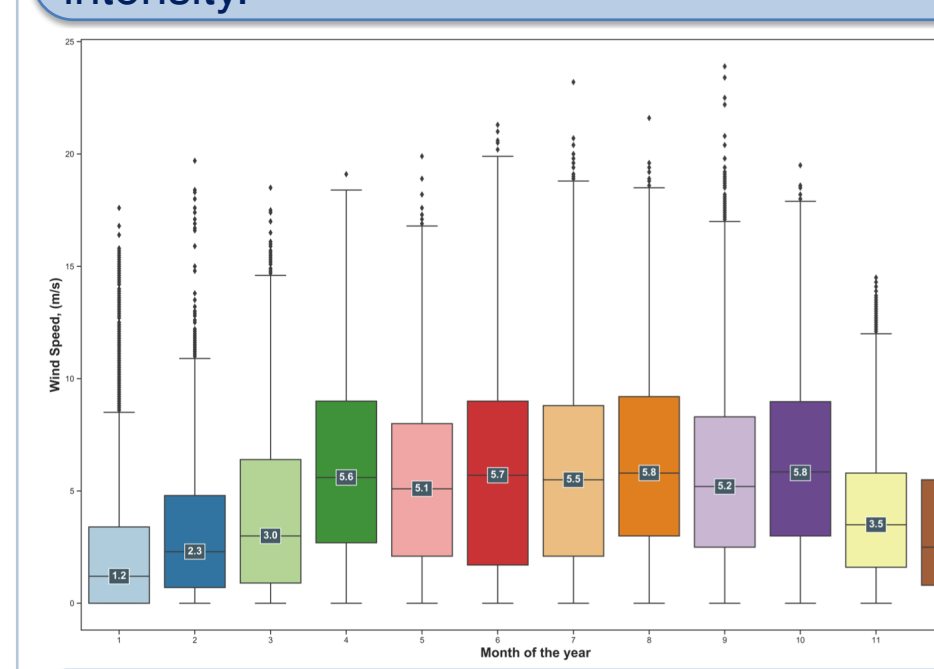


Fig. 18. Median wind values by month of the year in CP.

The impact of the winds on the DIQ are clearly represented in Fig. 16 and Fig. 17. When the winds become above 5 (m/s), the DIQ gets consistently deteriorated as shown in Fig. 17. Another case when DIQ degrades is while going to southerly positions in the sky with winds ranging 5 – 10 (m/s) and also for high winds (> 10 m/s) in northern positions.

On CP summit, the prevailing wind is coming from NW (30% of the time) and the most common wind speed is between 4 to 8 m/s. August and June are the windiest months of the year.

The Seeing Monitor

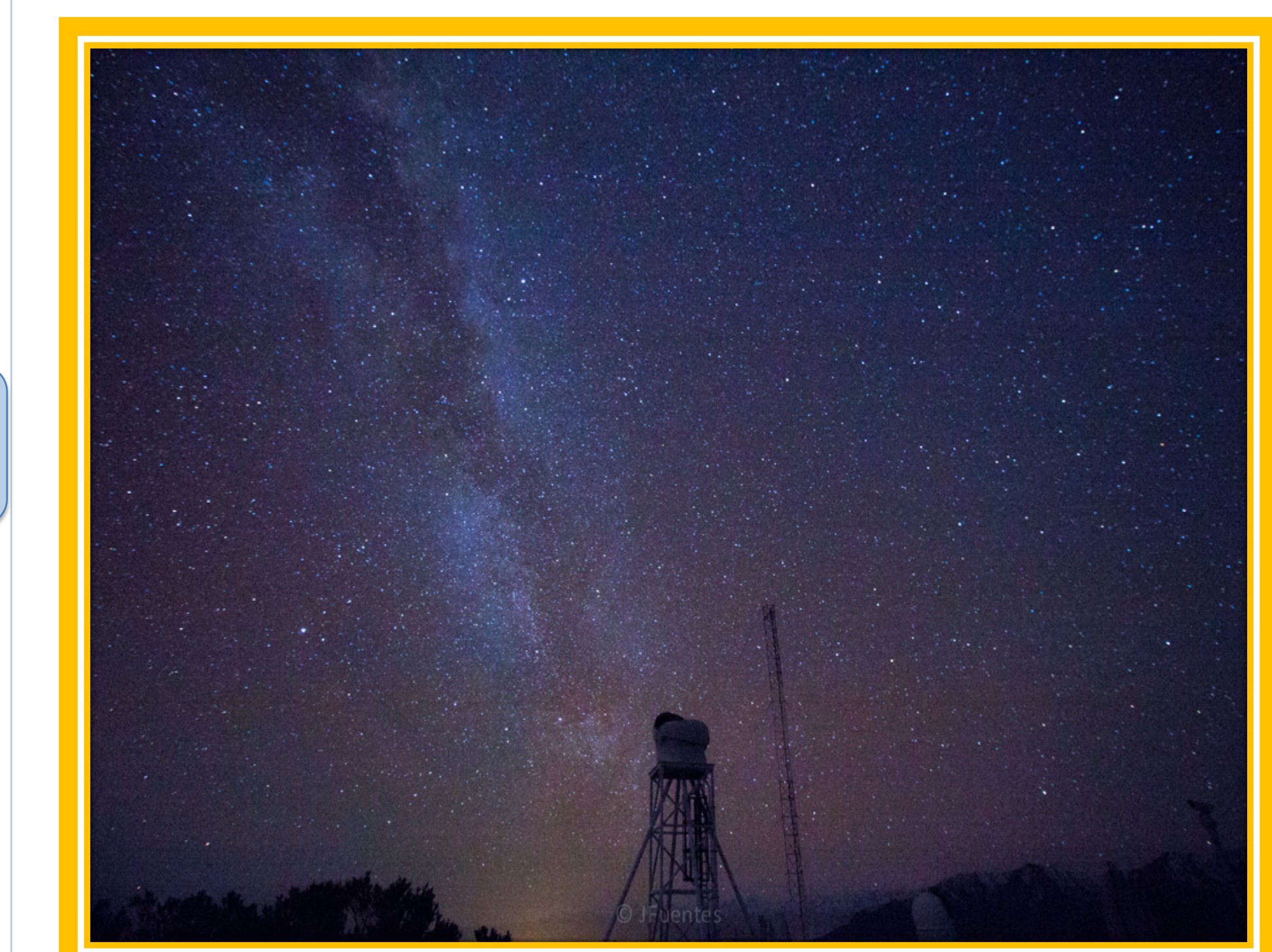


Fig. 20. Photography of the Seeing Monitor in the night sky at Cerro Pachón site.

REFERENCES

- Els, S. G. et al. 2009 PASP 121, 922.
- Tokovinin, A., 2002, PASP 114, 1156.
- Tokovinin A. & Travouillon T., 2006, MNRAS, 365, 1235.
- Martinez, P. et al. 2010, A&A, 516, A90.